A&A 579, A46 (2015)
DOI: 10.1051/0004-6361/201425478

Astronomy & Astrophysics

Millimeter and submillimeter wave spectra of mono-^{13}C-acetaldehydes⋆

L. Margulès[1], R. A. Motiyenko[1], V. V. Ilyushin[2], and J. C. Guillemin[3]

[1] Laboratoire de Physique des Lasers, Atomes, et Molécules, UMR CNRS 8523, Université de Lille I, 59655 Villeneuve d'Ascq Cedex, France
e-mail: laurent.margules@univ-lille1.fr
[2] Institute of Radio Astronomy of NASU, Chervonopraporna 4, 61002 Kharkov, Ukraine
e-mail: ilyushin@rian.kharkov.ua
[3] Institut des Sciences Chimiques de Rennes, École Nationale Supérieure de Chimie de Rennes, CNRS, UMR 6226, 11 allée de Beaulieu, CS 50837, 35708 Rennes Cedex 7, France

Received 6 December 2014 / Accepted 25 April 2015

ABSTRACT

Context. The acetaldehyde molecule is ubiquitous in the interstellar medium of our galaxy, and due to its dense and complex spectrum, large dipole moment, and several low-lying torsional states, acetaldehyde is considered to be a "weed" molecule for radio astronomy observations. Mono-^{13}C acetaldehydes $^{13}CH_3CHO$ and $CH_3{}^{13}CHO$ are likely to be identified in astronomical surveys, such as those available with the very sensitive ALMA telescope. Laboratory measurements and analysis of the millimeter and submillimeter-wave spectra are the prerequisites for the successful radioastronomical search for the new interstellar molecular species, as well as for new isotopologs of already detected interstellar molecules.

Aims. In this context, to provide reliable predictions of $^{13}CH_3CHO$ and $CH_3{}^{13}CHO$ spectra in millimeter and submillimeter wave ranges, we study rotational spectra of these species in the frequency range from 50 to 945 GHz.

Methods. The spectra of mono-^{13}C acetaldehydes were recorded using the spectrometer based on Schottky-diode frequency-multiplication chains in the Lille laboratory. The rotational spectra of $^{13}CH_3CHO$ and $CH_3{}^{13}CHO$ molecules were analyzed using the Rho axis method.

Results. In the recorded spectra we have assigned 6884 for the $^{13}CH_3CHO$ species and 6458 for $CH_3{}^{13}CHO$ species new rotational transitions belonging to the ground, first, and second excited torsional states. These measurements were fitted together with previously published data to the Hamiltonian models that use 91 and 87 parameters to achieve overall weighted rms deviations 0.88 for the $^{13}CH_3CHO$ species and 0.95 for $CH_3{}^{13}CHO$. On the basis of the new spectroscopic results, predictions of transition frequencies in the frequency range up to 1 THz with $J \leq 60$ and $K_a \leq 20$ are presented for both isotopologs.

Key words. ISM: molecules – methods: laboratory: molecular – submillimeter: ISM – molecular data – line: identification

1. Introduction

This paper is a continuation of a series of studies conducted in PhLAM Lille (France) that are devoted to the investigations of the spectra of different isotopic species of astrophysical molecules (Demyk et al. 2007; Margulès et al. 2009a,b, 2010; Carvajal et al. 2009; Tercero et al. 2012; Bouchez et al. 2012; Coudert et al. 2012, 2013; Richard et al. 2012, 2013; Haykal et al. 2013; Kutsenko et al. 2013; Nguyen et al. 2013). In particular, these works led to the first interstellar detection of $HCOOCH_2D$ (Coudert et al. 2013), $HCOO^{13}CH_3$ (Carvajal et al. 2009), $HCO^{18}OCH_3$, $HC^{18}OOCH_3$ (Tercero et al. 2012), and CH_2DOCH_3 (Richard et al. 2013). In the current paper we focus our attention on the ^{13}C isotopologs of the ubiquitous interstellar molecule – acetaldehyde, which main isotopolog has been observed in the cold molecular clouds (Matthews et al. 1985), and translucent molecular clouds (Turner et al. 1999) toward hot cores (Nummelin et al. 1998) and star-forming regions (Charnley 2004). It was recently detected in the disk of a high redshift ($z = 0.89$) spiral galaxy located in front of the quasar PKS 1830-211 (Muller et al. 2011).

Rotational spectra of the parent acetaldehyde species was a subject of several investigations. The latest paper on this subject (Smirnov et al. 2014) covers the frequency range up to 1.6 THz and the range of rotational quantum numbers up to $J \leq 66$ and $K_a \leq 22$, providing a firm basis for producing reliable predictions of the acetaldehyde spectrum in the frequency range up to 1.9 THz. As concerns mono-labeled acetaldehyde isotopolog, the millimeter and submillimeter wave spectra were only studied for CH_3CDO (Martinache et al. 1989; Elkeurti et al. 2010) with the upper frequency of 376 GHz. For other mono-substituted isotopologs CH_2DCHO, $^{13}CH_3CHO$, $CH_3{}^{13}CHO$, and $CH_3CH^{18}O$, data available in the literature are very limited, covering the frequency range only from 8 to 40 GHz (Kilb et al. 1957; Turner & Cox 1976; Turner et al. 1981; Zaleski et al. 2012). In particular, for the $^{13}CH_3CHO$ and $CH_3{}^{13}CHO$ isotopologs of interest here, the dataset consisted of about 10 transitions for each of the ^{13}C isotopologs, which are evenly distributed between A-type and E-type symmetry species of the ground torsional states (Kilb et al. 1957; Zaleski et al. 2012). It is evident that for producing reliable predictions of the $^{13}CH_3CHO$ and $CH_3{}^{13}CHO$ spectra, these datasets should be considerably extended and a new analysis should be performed. In this context we present a new study of the $^{13}CH_3CHO$ and $CH_3{}^{13}CHO$ spectra with measurements and analysis extended up to 945 GHz.

⋆ Full Tables 3–6 are only available at the CDS via anonymous ftp to cdsarc.u-strasbg.fr (130.79.128.5) or via http://cdsarc.u-strasbg.fr/viz-bin/qcat?J/A+A/579/A46

2. Experiments

2.1. Synthesis

The 1-^{13}C and 2-^{13}C acetyl chloride were purchased from Eurisotop and used without further purification. The $^{13}CH_3CHO$ and $CH_3{}^{13}CHO$ were synthesized following the preparation of Barbry and Couturier (Barbry et al. 1987), modified to isolate the product. In a 100 ml two-necked flask equipped with a stirring bar and a nitrogen inlet, and cooled at −20 °C were introduced under nitrogen $(PPh_3)_4Pd$ (0.12 g, 0.1 mmol), xylene (15 ml), and ^{13}C acetyl chloride (1g, 13 mmol). The flask was connected to a U-tube equipped with stopcocks and immersed in a −80 °C cold bath, and tributyl tin hydride (4.1 g, 14 mmol) was added in 2 min and the solution was then allowed to warm to room temperature. A gentle stream of nitrogen was then passed through the flask and the U-tube for 15 min. A mixture containing the labeled acetaldehyde (80%) and xylene (20%) was obtained. A very pure sample of ^{13}C acetaldehyde (purity >96%) was obtained in a 78% yield (437 mg, 10 mmol) and in a 98% isotopic purity by a subsequent distillation of the solution in a vacuum line (0.1 mbar) equipped with a first U-tube cooled at −80 °C to remove the solvent and a second one immersed in a liquid nitrogen bath to selectively condense the expected product.

2.2. Lille – submillimeter spectra

The measurements in the frequency range under investigation (50–945 GHz) were performed using the Lille spectrometer (Alekseev et al. 2012). A quasi-optic dielectric hollow waveguide of 3-m length containing investigated gas at the required pressure was used as the sample cell in the spectrometer. The measurements were done at typical pressures of 10 Pa and at room temperature. The frequency ranges 50–315, 400–630, and 780–945 GHz were covered with various active and passive frequency multipliers where the Agilent synthesizer (12.5–17.5 GHz) was used as the source of radiation. Estimated uncertainties for measured line frequencies are 30 kHz and 50 kHz depending on the observed signal-to-noise ratio and the frequency range.

3. Theoretical model

Like the parent species, ^{13}C acetaldehydes represent the case of near prolate ($\kappa \approx -0.95$) nonrigid molecules with the large amplitude torsional motion of the methyl top. The molecules have a plane of symmetry that means that the G_6 permutation-inversion group will be appropriate for them if internal rotation of the methyl group is taken into account. The torsional large amplitude motion of the methyl top in the molecules splits rotational transitions into two components that correspond to non-degenerate (A_1/A_2) and degenerate (E) symmetry species in G_6. Corresponding $A - E$ splittings may already reach hundreds of MHz in the ground vibrational state. Combination of rather large rotational constants ($A \approx 56$ GHz, $B \approx 10$ GHz, $C \approx 9$ GHz) with an intermediate barrier height to internal rotation of the methyl group ($V_3 \approx 407$ cm^{-1}) and considerable dipole moment ($\mu \approx 2.734$ D) leads to an intense complex rotational spectrum expanding in THz region. The ratio of the methyl top moment of inertia to that of the rest of the molecule is rather high in these molecules, which leads to a relatively large coefficient for the coupling term between internal rotation and global rotation ($\rho \approx 0.32$). This means that the principle axis method will experience serious problems with fitting spectra of ^{13}C acetaldehydes since its convergence strongly depends on the ρ value (Kleiner 2010).

The Hamiltonian used in the present work is the so-called RAM (rho axis method) internal-rotation Hamiltonian based on the work of Kirtman (Kirtman 1962), Lees and Baker (Lees & Baker 1968), and Herbst et al. (Herbst et al. 1984). Since rather complete descriptions of this method, which takes its name from the choice of axis system, have been presented several times (Hougen et al. 1994; Kleiner 2010) we do not repeat this general description here. The main advantage of the RAM Hamiltonian is its general approach that simultaneously takes into account the A- and E-symmetry species and all the torsional levels, intrinsically taking the intertorsional interactions into account within the rotation-torsion manifold of energy levels. This method was successfully applied to a number of molecules containing a C_{3v} rotor and C_s frame, including the main isotopolog of acetaldehyde (Smirnov et al. 2014). As for the main isotopolog (Smirnov et al. 2014) we employed the RAM36 (rho-axis-method for 3- and 6-fold barriers) code that uses the RAM approach for the molecules with the C_{3v} top attached to a molecular frame of C_s or C_{2v} symmetry and having 3- or 6-fold barriers to internal rotation, respectively (Ilyushin et al. 2010, 2013). The Hamiltonian in the RAM36 program is presented by the following expression:

$$\begin{aligned} H \;=\; & (1/2)\sum_{knpqrs} B_{knpqrs0}\left[P^{2k}P_z^nP_x^pP_y^qp_\alpha^r\cos(3s\alpha)\right. \\ & \left.+\cos(3s\alpha)p_\alpha^rP_y^qP_x^pP_z^nP^{2k}\right] \\ & +(1/2)\sum_{knpqrt} B_{knpqr0t}\left[P^{2k}P_z^nP_x^pP_y^qp_\alpha^r\sin(3t\alpha)\right. \\ & \left.+\sin(3t\alpha)p_\alpha^rP_y^qP_x^pP_z^nP^{2k}\right] \end{aligned} \quad (1)$$

where the $B_{knpqrst}$ are fitting parameters; p_α is the angular momentum conjugate to the internal rotation angle α; and P_x, P_y, P_z are projections on the x, y, z axes of the total angular momentum P. In the case of a C_{3v} top and C_s frame (as is appropriate for acetaldehyde), the allowed terms in the torsion-rotation Hamiltonian must be totally symmetric in the group G_6 (and also must be Hermitian and invariant to the time reversal operation). Since all individual operators $p_\alpha, P_x, P_y, P_z, P^2, \cos(3s\alpha)$ and $\sin(3t\alpha)$ used in Eq. (1) are Hermitian, all possible terms provided by Eq. (1) will automatically be Hermitian. The particular term to be fit is represented in the input file with a set of k, n, p, q, r, s, t integer indices that are checked by the program for conformity with time reversal and symmetry requirements, to prevent accidental introduction of symmetry-forbidden terms into the Hamiltonian.

The RAM36 computer code uses the two-step diagonalization procedure of Herbst et al. (1984). In the first step, a set of torsional calculations is performed with a relatively large torsional basis set for each symmetry species and for each value of K in the range $-J_{\max} \le K \le +J_{\max}$. In the current fit we used 21 torsional basis functions at the first stage. In this step only the main torsional-rotation Hamiltonian matrix elements diagonal in K are considered. In the second step a reduced torsional basis set is used, which is obtained by discarding all but the lowest several torsional eigenfunctions for a given K and symmetry species obtained from the first stage. In the current fit we used 9 torsional basis functions at the second stage. In the second step, all desired asymmetric-rotor and torsion-rotation K mixing effects are taken into account. At both stages a non-degenerate symmetry submatrix is not split into A_1/A_2 parts, which are instead treated together. A conventional weighted least-squares fit is carried out to determine the Hamiltonian parameter values

Table 1. Fitted parameters of the RAM Hamiltonian for ^{13}C acetaldehyde isotopologs.

Operator[1]	n_{tr}^2	Parameter	$^{12}CH_3{}^{12}CHO$ Value[3] (cm^{-1})	$^{13}CH_3{}^{12}CHO$ Value[3] (cm^{-1})	$^{12}CH_3{}^{13}CHO$ Value[3] (cm^{-1})
$p_\alpha{}^2$	2_{20}	F	7.56708175(35)	7.5652791(19)	7.5068034(55)
$(1/2)\,(1-\cos(3\alpha))$	2_{20}	V_3	407.59768(20)	407.91172(18)	407.58042(26)
$p_\alpha P_a$	2_{11}	ρ	0.328632673(20)	0.328300981(35)	0.322541154(65)
$P_a{}^2$	2_{02}	A_{RAM}	1.884881309(61)	1.88013742(13)	1.848976496(63)
$P_b{}^2$	2_{02}	B_{RAM}	0.348706489(16)	0.337726802(58)	0.348720666(61)
$P_c{}^2$	2_{02}	C_{RAM}	0.3031840478(44)	0.294817724(11)	0.302179145(18)
$\{P_a,P_b\}$	2_{02}	D_{ab}	−0.122669037(94)	−0.11817144(38)	−0.12175149(39)
$(1/2)\,(1-\cos(6\alpha))$	4_{40}	V_6	−11.63964(50)	−11.67172(20)	−11.71571(65)
$p_\alpha{}^4$	4_{40}	F_m	$-0.424416(38)\times10^{-3}$	$-0.427829(96)\times10^{-3}$	$-0.42834(12)\times10^{-3}$
$p_\alpha{}^3P_a$	4_{31}	ρ_m	$-0.832163(52)\times10^{-3}$	$-0.82821(11)\times10^{-3}$	$-0.81162(16)\times10^{-3}$
$P^2(1-\cos(3\alpha))$	4_{22}	V_{3J}	$0.5577894(41)\times10^{-3}$	$0.524776(16)\times10^{-3}$	$0.529795(22)\times10^{-3}$
$P_a{}^2(1-\cos(3\alpha))$	4_{22}	V_{3K}	$-0.19313906(98)\times10^{-1}$	$-0.1898291(17)\times10^{-1}$	$-0.1953217(29)\times10^{-1}$
$(P_b{}^2-P_c{}^2)(1-\cos(3\alpha))$	4_{22}	V_{3bc}	$0.2114597(52)\times10^{-3}$	$0.192215(19)\times10^{-3}$	$0.213208(15)\times10^{-3}$
$(1/2)\{P_a,P_b\}(1-\cos(3\alpha))$	4_{22}	V_{3ab}	$0.4235363(70)\times10^{-2}$	$0.405222(33)\times10^{-2}$	$0.443922(36)\times10^{-2}$
$p_\alpha{}^2P^2$	4_{22}	F_J	$-0.291704(53)\times10^{-5}$	$-0.26533(11)\times10^{-5}$	$-0.31536(19)\times10^{-5}$
$p_\alpha{}^2P_a{}^2$	4_{22}	F_K	$-0.982545(30)\times10^{-3}$	$-0.972792(46)\times10^{-3}$	$-0.944979(89)\times10^{-3}$
$p_\alpha{}^2(P_b{}^2-P_c{}^2)$	4_{22}	F_{bc}	$0.14720(12)\times10^{-5}$	$0.13745(31)\times10^{-5}$	$0.16632(37)\times10^{-5}$
$(1/2)\{P_a,P_c\}\sin(3\alpha)$	4_{22}	D_{3ac}	$-0.1405503(49)\times10^{-1}$	$-0.135881(17)\times10^{-1}$	$-0.142957(18)\times10^{-1}$
$(1/2)\{P_b,P_c\}\sin(3\alpha)$	4_{22}	D_{3bc}	$0.59173(13)\times10^{-3}$	$0.55489(43)\times10^{-3}$	$0.63859(48)\times10^{-3}$
$p_\alpha P_a P^2$	4_{13}	ρ_J	$0.958253(42)\times10^{-5}$	$0.91984(11)\times10^{-5}$	$0.91075(15)\times10^{-5}$
$p_\alpha P_a{}^3$	4_{13}	ρ_K	$-0.571407(12)\times10^{-3}$	$-0.564681(12)\times10^{-3}$	$-0.549548(31)\times10^{-3}$
$(1/2)\{P_a,(P_b{}^2-P_c{}^2)\}p_\alpha$	4_{13}	ρ_{bc}	$-0.5536(12)\times10^{-6}$	$-0.5763(36)\times10^{-6}$	$-0.2887(35)\times10^{-6}$
$-P^4$	4_{04}	Δ_J	$0.3244101(54)\times10^{-6}$	$0.306742(20)\times10^{-6}$	$0.325255(24)\times10^{-6}$
$-P^2P_a{}^2$	4_{04}	Δ_{JK}	$-0.581770(50)\times10^{-5}$	$-0.556079(86)\times10^{-5}$	$-0.571647(79)\times10^{-5}$
$-P_a{}^4$	4_{04}	Δ_K	$0.1308173(26)\times10^{-3}$	$0.1292582(29)\times10^{-3}$	$0.1263888(56)\times10^{-3}$
$-2P^2(P_b{}^2-P_c{}^2)$	4_{04}	δ_J	$0.778472(23)\times10^{-7}$	$0.709225(70)\times10^{-7}$	$0.786517(69)\times10^{-7}$
$-\{P_a{}^2,(P_b{}^2-P_c{}^2)\}$	4_{04}	δ_K	$0.94268\ (17)\times10^{-6}$	$0.105094(90)\times10^{-5}$	$0.10255(12)\times10^{-5}$
$\{P_a,P_b\}P^2$	4_{04}	D_{abJ}	$0.867443(32)\times10^{-6}$	$0.81273(20)\times10^{-6}$	$0.85179(14)\times10^{-6}$
$\{P_a{}^3,P_b\}$	4_{04}	D_{abK}	$0.30498(25)\times10^{-5}$	$0.29239(46)\times10^{-5}$	$0.27116(33)\times10^{-5}$

Notes. [(1)] $\{A,B\}=AB+BA$; $\{A,B,C\}=ABC+CBA$; $\{A,B,C,D\}=ABCD+DCBA$. The product of the operator in the first column of a given row and the parameter in the third column of that row gives the term actually used in the torsion-rotation Hamiltonian of the program, except for F, ρ, and A_{RAM}, which occur in the Hamiltonian in the form $F(P_\alpha+\rho P_a)^2+A_{RAM}P_a^2$. [(2)] $n=t+r$, where n is the total order of the operator, t is the order of the torsional part, and r the order of the rotational part. [(3)] All values are in cm^{-1}, except ρ, which is unitless. Statistical uncertainties are shown as one standard uncertainty in the units of the last two digits. A complete version up to 8th order is available in Table 7.

with a special treatment of blends where an intensity-weighted average of calculated (but experimentally unresolved) transition frequencies is put in correspondence with the measured blended-line frequency. A more detailed description of the RAM36 code can be found in Ilyushin et al. (2010, 2013).

4. Assignment and analysis of the spectra

We started our analysis of recorded spectra from the dataset of Kilb et al. (1957), which was combined with the low order torsion parameters of the main acetaldehyde isotopolog (Smirnov et al. 2014). In the initial stage the torsional parameters of the RAM Hamiltonian models were kept fixed at the values of the main isotopolog, and rotational parameters plus ρ parameters were varied to fit available transitions of $^{13}CH_3CHO$ and $CH_3{}^{13}CHO$. Obtained in this way sets of RAM Hamiltonian parameters were used to produce the initial predictions of millimeter and submillimeter wave spectra for both ^{13}C isotopologs. Analysis of the recorded spectra was done in the usual iterative manner by adding new assigned lines to the fit, refining of Hamiltonian model, and producing new predictions.

Although from the point of view of future radio astronomy observations, we were mainly interested in the rotational transitions belonging to the ground torsional states of ^{13}C acetaldehydes, several transitions belonging to the first and second excited torsional states have also been assigned. The band origins of the excited torsional states are $\nu^A=143.7836\ cm^{-1}$, $\nu^E=142.0401\ cm^{-1}$ ($v_t=1$), $\nu^A=255.3495\ cm^{-1}$, and $\nu^E=269.2086\ cm^{-1}$ ($v_t=2$) for $^{13}CH_3CHO$, and $\nu^A=143.1719\ cm^{-1}$, $\nu^E=141.4820\ cm^{-1}$ ($v_t=1$) $\nu^A=254.6352\ cm^{-1}$, and $\nu^E=268.1986\ cm^{-1}$ ($v_t=2$) for $CH_3{}^{13}CHO$. First of all the excited torsional states were added to the analysis to stabilize the fit and reduce the correlation between torsion parameters of the RAM Hamiltonian models. In addition several high-K_a series of the ground torsional state transitions were perturbed by interactions with the first and second excited torsional states, so it was necessary to get more precise information about the positions of energy levels of these states.

In total the new datasets for the rotational spectra of $^{13}CH_3CHO$ and $CH_3{}^{13}CHO$ isotopologs include 6894 and 6465 measured line frequencies, respectively, with an upper value of $J=60$. As already mentioned, both datasets include transitions belonging to the ground, first, and second excited torsional states of the ^{13}C acetaldehyde isotopologs. These sets of rotational transitions were fitted to the RAM theoretical model described above. The fits adopted in the present study as the best achieved the root mean square (rms) deviations of 0.032 MHz for $^{13}CH_3CHO$ and 0.034 MHz for $CH_3{}^{13}CHO$. The weighted rms deviations for the fits were 0.88 and 0.95, respectively. The RAM Hamiltonian models include 91 parameters for $^{13}CH_3CHO$ and 87 for $CH_3{}^{13}CHO$. The values of the molecular parameters obtained from the final fits are presented in Table 1,

Table 2. Statistics of the data set for the global fit to v_t = 0, 1, 2 torsional states of $^{13}CH_3CHO$ and $CH_3{}^{13}CHO$ isotopologs of acetaldehyde molecule.

$^{13}CH_3CHO$			$CH_3{}^{13}CHO$		
Category[1]	# of transitions[2]	rms[3]	Category[1]	# of transitions[2]	rms[3]
v_t = 0 A-type	2277	0.034 MHz	v_t = 0 A-type	2246	0.033 MHz
v_t = 0 E-type	2439	0.031 MHz	v_t = 0 E-type	2304	0.035 MHz
v_t = 1 A-type	1144	0.032 MHz	v_t = 1 A-type	1062	0.031 MHz
v_t = 1 E-type	1118	0.029 MHz	v_t = 1 E-type	1071	0.034 MHz
v_t = 2 A-type	331	0.033 MHz	v_t = 2 A-type	296	0.033 MHz
v_t = 2 E-type	383	0.036 MHz	v_t = 2 E-type	294	0.046 MHz
Unc.[4]	# of lines[2]	rms[3]	Unc.[4]	# of lines[2]	rms[3]
0.030 MHz	5377	0.027 MHz	0.030 MHz	5111	0.029 MHz
0.050 MHz	1507	0.041 MHz	0.050 MHz	1347	0.047 MHz
0.100 MHz	3	0.127 MHz	0.200 MHz	4	0.231 MHz
0.200 MHz	4	0.286 MHz	0.300 MHz	2	0.067 MHz
0.300 MHz	2	0.137 MHz	0.500 MHz	1	0.262 MHz
0.500 MHz	1	0.191 MHz			

Notes. [(1)] The transitions are grouped by symmetry and torsional quantum number v_t. [(2)] The number of transitions or measured lines in each category included in the least squares fit. Due to blending, the total number of assigned transitions differs from the total number of measured lines. [(3)] Root-mean-square deviations from the global fit. [(4)] Data are grouped by their assigned uncertainties in the fit. Weights used for all lines in the fit are $1/(\text{unc.})^2$.

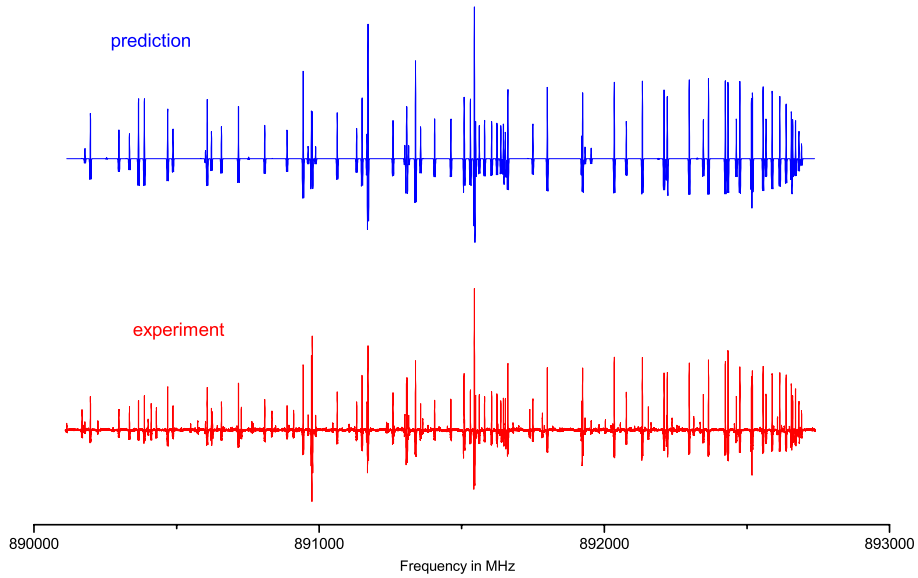

Fig. 1. Predicted (in blue) and observed (in red) rotational spectrum of $^{13}CH_3CHO$ between 891.3 and 893.2 GHz dominated by Q-type series of transitions with $K_a = 10 \leftarrow 9$. A slight inconsistency between predicted and observed spectrum, which may be visible for some strong lines, is due to source power and detector sensitivity variations.

where they are compared with the parameters of the main isotopolog Smirnov et al. (2014; owing to its significant size, the complete version of Table 1 is presented in Table 7), here only the parameters up to fourth order are given. It is seen from the comparison that up to the fourth order the RAM Hamiltonian models for the ^{13}C isotopologs are very close to the corresponding model of the main isotopolog. Starting from the sixth order, some discrepancies in the sets of parameters begin to appear. In our opinion these discrepancies are caused by the differences in the datasets. For example, the far-infrared data on the fundamental torsional band is only available for the main acetaldehyde isotopolog. The $K_a = 9 \leftarrow 8$ Q series of lines presented at Fig. 1 of Smirnov et al. (2014) may serve as one more example of such differences in the datasets: this series of transitions is present in the datasets of $^{12}CH_3{}^{12}CHO$ and $^{13}CH_3{}^{12}CHO$, but is out of range of the Lille spectrometer for $^{12}CH_3{}^{13}CHO$.

Table 2 summarizes the fitting results for different groups of the data. It is seen that the two main groups of data with 0.030 MHz and 0.050 MHz uncertainties are fit within the experimental error. The separate rms deviations for the A and E symmetry species are close to each other and do not differ much between torsional excited states. Figures 1 and 2, in which observed and predicted spectra are compared, give additional illustrations of our current understanding of the ^{13}C acetaldehydes spectra. The regions of the Q series of $K_a = 10 \leftarrow 9$ transitions are presented in these figures. It is seen that the majority of strong lines are assigned and predicted by our current model, although a number of rather strong unassigned lines presumably belonging to the higher excited states may still be found in the experimental spectra.

The lists of measured rotational transitions of the $^{13}CH_3CHO$ and $CH_3{}^{13}CHO$ isotopologs are presented in Tables 3 and 4.

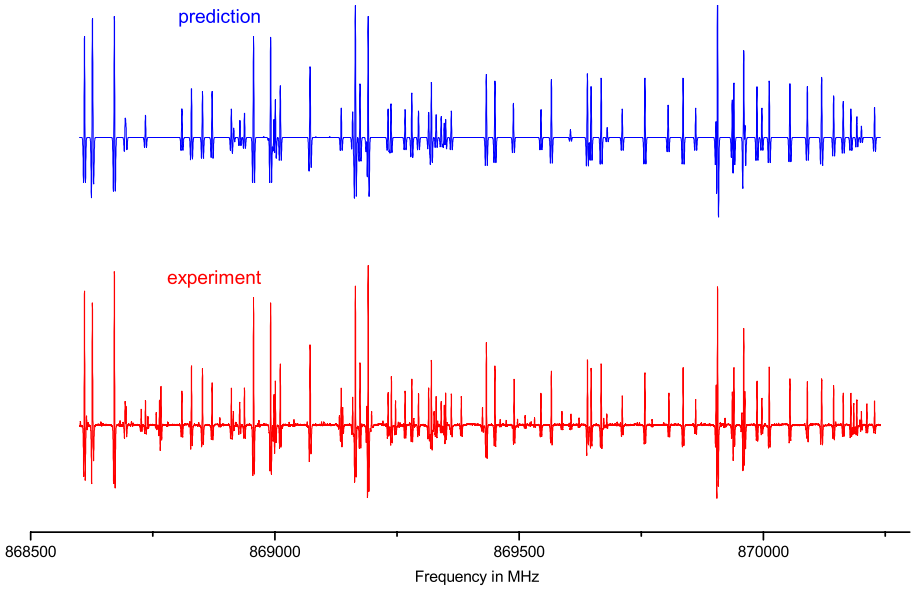

Fig. 2. Predicted (in blue) and observed (in red) rotational spectrum of $CH_3{}^{13}CHO$ between 869.3 and 871.0 GHz dominated by Q-type series of transitions with $K_a = 10 \leftarrow 9$. A slight inconsistency between predicted and observed spectrum, which may be visible for some strong lines, is due to source power and detector sensitivity variations.

Table 3. Assignments, measured transition frequencies, and residuals from the global fit of the microwave, millimeter-wave, and submillimeter-wave $v_t = 0,1,2$ data for $^{13}CH_3CHO$ acetaldehyde.

Upper level					Lower level					Position(Unc.)	O–C.	Source	Comment
Sy	v_t	J	K_a	K_c	Sy	v_t	J	K_a	K_c	(in MHz)	(in MHz)		
$A1$	0	3	1	2	$A2$	0	3	0	3	50 499.1760(0.0500)	−0.0005		
$A2$	0	4	1	3	$A1$	0	4	0	4	52 643.0560(0.0500)	0.0111		
$A1$	0	5	1	4	$A2$	0	5	0	5	55 411.1830(0.0500)	0.0129		
$A2$	0	6	1	5	$A1$	0	6	0	6	58 859.8770(0.0500)	0.0362		
$A1$	0	7	1	6	$A2$	0	7	0	7	63 052.9260(0.0500)	−0.0162		
$A2$	0	10	1	9	$A1$	0	10	0	10	80 776.1640(0.0500)	0.0373		
$A1$	0	13	1	12	$A2$	0	13	0	13	107 350.8210(0.0300)	−0.0171		
$A2$	0	14	1	13	$A1$	0	14	0	14	118 271.1660(0.0300)	0.0042		
$A1$	0	15	1	14	$A2$	0	15	0	15	130 175.9920(0.0300)	−0.0249		
$A2$	0	16	1	15	$A1$	0	16	0	16	142 998.5600(0.0300)	−0.0006		
$A1$	0	17	1	16	$A2$	0	17	0	17	156 649.3120(0.0300)	−0.0152		
$A2$	0	18	1	17	$A1$	0	18	0	18	171 020.7020(0.0300)	0.0011		
$A1$	0	19	1	18	$A2$	0	19	0	19	185 992.3500(0.0300)	−0.0246		
$A2$	0	20	1	19	$A1$	0	20	0	20	201 437.3930(0.0300)	0.0079		
$A2$	0	22	1	21	$A1$	0	22	0	22	233 243.5300(0.0300)	0.0439		
$A1$	0	23	1	22	$A2$	0	23	0	23	249 371.9770(0.0300)	0.0040		
$A2$	0	24	1	23	$A1$	0	24	0	24	265 518.1390(0.0300)	−0.0019		
$A1$	0	25	1	24	$A2$	0	25	0	25	281 604.1520(0.0300)	0.0042		
$A2$	0	26	1	25	$A1$	0	26	0	26	297 570.9590(0.0300)	0.0110		
$A1$	0	27	1	26	$A2$	0	27	0	27	313 377.6680(0.0300)	0.0153		
$A1$	0	33	1	32	$A2$	0	33	0	33	404 255.7570(0.0300)	−0.0218		
$A2$	0	34	1	33	$A1$	0	34	0	34	418 806.7790(0.0300)	0.0311		
$A1$	0	35	1	34	$A2$	0	35	0	35	433 225.8170(0.0300)	0.0342		
$A2$	0	36	1	35	$A1$	0	36	0	36	447 527.9000(0.0300)	0.0275		
$A1$	0	37	1	36	$A2$	0	37	0	37	461 726.8520(0.0300)	0.0298		
$A2$	0	38	1	37	$A1$	0	38	0	38	475 835.0620(0.0300)	0.0353		
$A1$	0	39	1	38	$A2$	0	39	0	39	489 863.4180(0.0300)	0.0186		
$A2$	0	40	1	39	$A1$	0	40	0	40	503 821.4490(0.0300)	0.0469		
$A1$	0	41	1	40	$A2$	0	41	0	41	517 717.2310(0.0300)	0.0952		
$A1$	0	43	1	42	$A2$	0	43	0	43	545 348.1920(0.0300)	0.0406		
$A2$	0	44	1	43	$A1$	0	44	0	44	559 094.0470(0.0300)	0.0473		
$A1$	0	45	1	44	$A2$	0	45	0	45	572 799.0380(0.0300)	0.0567		
$A1$	0	47	1	46	$A2$	0	47	0	47	600 098.8390(0.0300)	0.0426		
$A2$	0	48	1	47	$A1$	0	48	0	48	613 698.4900(0.0300)	0.0412		

Notes. Full table is available at the CDS: S3.

Table 4. Assignments, measured transition frequencies, and residuals from the global fit of the microwave, millimeter-wave, and submillimeter-wave $v_t = 0, 1, 2$ data for $CH_3{}^{13}CHO$ acetaldehyde.

Upper level					Lower level					Position(Unc.)	O–C	Source	Comment
Sy	v_t	J	K_a	K_c	Sy	v_t	J	K_a	K_c	(in MHz)	(in MHz)		
$A2$	0	1	0	1	$A1$	0	0	0	0	19 232.4300(0.3000)	0.0062	*KLW*	
$A1$	0	2	0	2	$A2$	0	1	0	1	38 445.3800(0.2000)	0.1300	*KLW*	
$A2$	0	3	0	3	$A1$	0	2	0	2	57 618.9420(0.0500)	0.0162		
$A1$	0	4	0	4	$A2$	0	3	0	3	76 734.0720(0.0500)	−0.0390		
$A2$	0	5	0	5	$A1$	0	4	0	4	95 772.0540(0.0500)	−0.0346		
$A1$	0	6	0	6	$A2$	0	5	0	5	114 715.5210(0.0500)	0.0103		
$A2$	0	7	0	7	$A1$	0	6	0	6	133 549.5330(0.0500)	0.0173		
$A1$	0	8	0	8	$A2$	0	7	0	7	152 263.1490(0.0500)	0.0081		
$A2$	0	9	0	9	$A1$	0	8	0	8	170 850.8080(0.0500)	0.0141		
$A1$	0	10	0	10	$A2$	0	9	0	9	189 313.4080(0.0500)	0.0120		
$A1$	0	12	0	12	$A2$	0	11	0	11	225 900.8640(0.0500)	0.0183		
$A2$	0	13	0	13	$A1$	0	12	0	12	244 058.0550(0.0500)	−0.0031		
$A1$	0	14	0	14	$A2$	0	13	0	13	262 150.7570(0.0500)	0.0104		
$A2$	0	15	0	15	$A1$	0	14	0	14	280 198.7740(0.0500)	0.0046		
$A1$	0	16	0	16	$A2$	0	15	0	15	298 219.5590(0.0500)	0.0070		
$A1$	0	22	0	22	$A2$	0	21	0	21	406 309.5330(0.0300)	0.0055		
$A2$	0	23	0	23	$A1$	0	22	0	22	424 350.6000(0.0300)	0.0013		
$A1$	0	24	0	24	$A2$	0	23	0	23	442 399.0100(0.0300)	0.0005		
$A2$	0	25	0	25	$A1$	0	24	0	24	460 453.4140(0.0300)	−0.0043		
$A1$	0	26	0	26	$A2$	0	25	0	25	478 512.4370(0.0300)	−0.0008		
$A2$	0	27	0	27	$A1$	0	26	0	26	496 574.7260(0.0300)	−0.0122		
$A1$	0	28	0	28	$A2$	0	27	0	27	514 639.0980(0.0300)	−0.0033		
$A2$	0	29	0	29	$A1$	0	28	0	28	532 704.4390(0.0300)	−0.0043		
$A1$	0	30	0	30	$A2$	0	29	0	29	550 769.8140(0.0300)	−0.0041		
$A2$	0	31	0	31	$A1$	0	30	0	30	568 834.4090(0.0300)	−0.0013		
$A1$	0	32	0	32	$A2$	0	31	0	31	586 897.5190(0.0300)	−0.0034		
$A2$	0	33	0	33	$A1$	0	32	0	32	604 958.5620(0.0300)	0.0024		
$A1$	0	34	0	34	$A2$	0	33	0	33	623 017.0230(0.0300)	0.0080		
$A2$	0	43	0	43	$A1$	0	42	0	42	785 371.2800(0.0500)	0.0459		
$A1$	0	44	0	44	$A2$	0	43	0	43	803 387.2720(0.0500)	0.0866		
$A2$	0	45	0	45	$A1$	0	44	0	44	821 397.8580(0.0500)	0.0490		
$A1$	0	46	0	46	$A2$	0	45	0	45	839 403.0260(0.0500)	0.0660		
$A1$	0	48	0	48	$A2$	0	47	0	47	875 395.8740(0.0500)	−0.4172		$b + 0.0002$
$A2$	0	49	0	49	$A1$	0	48	0	48	893 383.8740(0.0500)	−0.3303		$b - 0.0128$
$A1$	0	50	0	50	$A2$	0	49	0	49	911 365.8540(0.0500)	−0.2552		$b - 0.0139$
$A2$	0	51	0	51	$A1$	0	50	0	50	929 341.6450(0.0500)	−0.2336		$b - 0.0505$

Notes. Full table is available at the CDS: S4.

They include the transition frequencies obtained in this study, as well as those available from the previous study (Kilb et al. 1957). In the first ten columns of Tables 3 and 4, the labeling for each spectral line is given: symmetry, v_t, J, K_a, and K_c. In the following columns we provide the observed transition frequencies, measurement uncertainties, residuals from the fit, and the reference in the case of Kilb et al. (1957) data (column Source). The last column Comment provides differences between the intensity-weighted average of calculated (but experimentally unresolved) transition frequencies and the observed position of the cluster of blended lines (indicated by "b" in this column). The transitions in Tables 3 and 4 are grouped in series where transitions with the same symmetry, v_t, and K_a quantum numbers are sorted in ascending order by J quantum number. Owing to their large sizes, the complete versions of Tables (S3 and S4) are presented at the CDS. Here only parts of these tables are given for illustration purposes.

The predictions for the rotational spectra of the ground and first excited torsional states of the $^{13}CH_3CHO$ and $CH_3{}^{13}CHO$ isotopologs up to 1 THz are given in Tables 5 and 6. The spectra were calculated using the sets of RAM Hamiltonian parameters presented in Table 7. As in Tables 3 and 4, the first ten columns contain the labeling of transitions. The quantum numbers are followed by the columns with calculated transition frequencies and corresponding uncertainties. The next two columns contain the energy of the lower state in cm^{-1} and the product $\mu^2 S$, where μ is the dipole moment of the molecule and S a transition linestrength. In our calculations of the $^{13}CH_3CHO$ and $CH_3{}^{13}CHO$ spectra, the values for the dipole moment components were taken to be equal to the corresponding values of the parent acetaldehyde isotopolog (Smirnov et al. 2014). In predictions we have adopted the limitations on rotational quantum numbers of $J = 65, K_a = 20$. In Tables 5 and 6, those transitions that match the frequency range requirement (from 1 GHz to 1 THz), whose predicted uncertainties are less than 0.1 MHz, and line strengths exceeding the limit of 0.01 are included. The complete versions of these tables will also be presented at the CDS: S5 and S6. We provide in Table 8 the rotational parts of the partition functions $Q_r(T)$ for $^{13}CH_3CHO$ and $CH_3{}^{13}CHO$ calculated from first principles, i.e., via direct summation over the rotational-torsional states. The maximum

Table 5. List of calculated positions and assignments of A–A and E–E transitions in the v_t = 0,1 torsional states of $^{13}CH_3CHO$ acetaldehyde up to J = 65 in the 1–1000 GHz frequency range.

Upper level					Lower level					Position	Uncert.	E_{lower}	$\mu^2 * S$
Sy	v_t	J	K_a	K_c	Sy	v_t	J	K_a	K_c	(MHz)	(MHz)	cm^{-1}	D^2
$A1$	0	10	10	0	$A2$	0	10	9	2	892 691.6257	(0.0060)	161.4200	$0.112 \times 10^{+1}$
$A2$	0	10	10	1	$A1$	0	10	9	1	892 691.6257	(0.0060)	161.4200	$0.112 \times 10^{+1}$
E	0	20	10	10	E	0	20	9	12	892 743.8813	(0.0044)	258.2060	$0.951 \times 10^{+1}$
E	1	34	10	24	E	1	34	9	25	892 777.0896	(0.0279)	640.3145	$0.191 \times 10^{+2}$
E	0	19	10	9	E	0	19	9	11	892 818.1797	(0.0045)	245.7254	$0.877 \times 10^{+1}$
E	0	18	10	8	E	0	18	9	10	892 884.0773	(0.0046)	233.8688	$0.803 \times 10^{+1}$
E	0	41	10	32	E	0	42	8	35	892 904.9678	(0.0126)	664.2723	0.181×10^{-1}
E	1	20	61	4	E	1	19	5	14	892 920.7693	(0.0057)	301.0407	$0.897 \times 10^{+1}$
E	0	17	10	7	E	0	17	9	9	892 942.2879	(0.0047)	222.6363	$0.727 \times 10^{+1}$
E	0	16	10	6	E	0	16	9	8	892 993.4892	(0.0048)	212.0279	$0.649 \times 10^{+1}$
E	0	15	10	5	E	0	15	9	7	893 038.3229	(0.0050)	202.0436	$0.569 \times 10^{+1}$
E	1	16	71	0	E	1	15	6	10	893 071.5613	(0.0064)	273.2469	$0.878 \times 10^{+1}$
E	0	14	10	4	E	0	14	9	6	893 077.3943	(0.0051)	192.6833	$0.486 \times 10^{+1}$
E	0	10	8	3	E	0	9	7	3	893 089.1803	(0.0045)	105.0124	$0.882 \times 10^{+1}$
E	0	13	10	3	E	0	13	9	5	893 111.2722	(0.0053)	183.9471	$0.400 \times 10^{+1}$
E	0	12	10	2	E	0	12	9	4	893 140.4887	(0.0055)	175.8349	$0.310 \times 10^{+1}$
$A2$	0	48	44	5	$A1$	0	47	4	44	893 144.1811	(0.0044)	729.9167	$0.300 \times 10^{+3}$
E	0	11	10	1	E	0	11	9	3	893 165.5391	(0.0056)	168.3467	$0.214 \times 10^{+1}$
E	0	48	44	5	E	0	47	4	44	893 173.5666	(0.0044)	729.9087	$0.300 \times 10^{+3}$
E	0	10	10	0	E	0	10	9	2	893 186.8816	(0.0058)	161.4826	$0.112 \times 10^{+1}$

Notes. Full table is available at the CDS: S5.

Table 6. List of calculated positions and assignments of A–A and E–E transitions in the v_t = 0,1 torsional states of $CH_3{}^{13}CHO$ acetaldehyde up to J = 65 in the 1–1000 GHz frequency range.

Upper level					Lower level					Position	Uncert.	E_{lower}	$\mu^2 * S$
Sy	v_t	J	K_a	K_c	Sy	v_t	J	K_a	K_c	(MHz)	(MHz)	cm^{-1}	D^2
$A1$	0	18	10	8	$A2$	0	18	9	10	870 012.2402	(0.0059)	233.6446	$0.788 \times 10^{+1}$
$A2$	0	18	10	9	$A1$	0	18	9	9	870 012.2402	(0.0059)	233.6446	$0.788 \times 10^{+1}$
$A1$	0	17	10	7	$A2$	0	17	9	9	870 054.6472	(0.0060)	222.0937	$0.713 \times 10^{+1}$
$A2$	0	17	10	8	$A1$	0	17	9	8	870 054.6472	(0.0060)	222.0937	$0.713 \times 10^{+1}$
E	0	45	7	38	E	0	44	7	38	870 090.1522	(0.0037)	711.3277	$0.861 \times 10^{+1}$
$A1$	0	16	10	6	$A2$	0	16	9	8	870 090.2612	(0.0062)	211.1846	$0.637 \times 10^{+1}$
$A2$	0	16	10	7	$A1$	0	16	9	7	870 090.2612	(0.0062)	211.1846	$0.637 \times 10^{+1}$
E	0	22	10	12	E	0	22	9	14	870 118.9446	(0.0053)	286.3095	$0.108 \times 10^{+1}$
$A1$	0	15	10	5	$A2$	0	15	9	7	870 119.8492	(0.0064)	200.9173	$0.558 \times 10^{+1}$
$A2$	0	15	10	6	$A1$	0	15	9	6	870 119.8492	(0.0064)	200.9173	$0.558 \times 10^{+1}$
$A1$	0	14	10	4	$A2$	0	14	9	6	870 144.1309	(0.0066)	191.2918	$0.477 \times 10^{+1}$
$A2$	0	14	10	5	$A1$	0	14	9	5	870 144.1309	(0.0066)	191.2918	$0.477 \times 10^{+1}$
$A1$	0	13	10	3	$A2$	0	13	9	5	870 163.7793	(0.0068)	182.3081	$0.392 \times 10^{+1}$
$A2$	0	13	10	4	$A1$	0	13	9	4	870 163.7793	(0.0068)	182.3081	$0.392 \times 10^{+1}$
$A1$	0	12	10	2	$A2$	0	12	9	4	870 179.4213	(0.0070)	173.9662	$0.304 \times 10^{+1}$
$A2$	0	12	10	3	$A1$	0	12	9	3	870 179.4213	(0.0070)	173.9662	$0.304 \times 10^{+1}$
$A1$	0	11	10	1	$A2$	0	11	9	3	870 191.6377	(0.0072)	166.2659	$0.210 \times 10^{+1}$
$A2$	0	11	10	2	$A1$	0	11	9	2	870 191.6377	(0.0072)	166.2659	$0.210 \times 10^{+1}$
$A1$	0	10	10	0	$A2$	0	10	9	2	870 200.9637	(0.0074)	159.2075	$0.110 \times 10^{+1}$
$A2$	0	10	10	1	$A1$	0	10	9	1	870 200.9637	(0.0074)	159.2075	$0.110 \times 10^{+1}$

Notes. Full table is available at the CDS: S6.

value of the J quantum number for the energy levels taken for calculating the partition function is 100. The vibrational part $Q_v(T)$ may be estimated in the harmonic approximation using the normal modes reported for the main isotopolog of acetaldehyde by Schimanouchi (1972). Simple formulas for calculating $Q_v(T)$ can be found elsewhere (see, for example, Gordy & Cook 1984).

5. Conclusion

A new study of the rotational spectra of the $^{13}CH_3CHO$ and $CH_3{}^{13}CHO$ isotopologs of the acetaldehyde molecule was carried out in a wide frequency range up to 945 GHz. The study represents more than a twenty-fold expansion in terms of frequency range coverage for the rotational spectra of mono-^{13}C

Table 7. Fitted parameters of the RAM Hamiltonian for ^{13}C acetaldehyde isotopologs.

Operator[1]	n_{tr}[2]	Parameter	$^{12}CH_3{}^{12}CHO$ value[3] (cm^{-1})	$^{13}CH_3{}^{12}CHO$ value[3] (cm^{-1})	$^{12}CH_3{}^{13}CHO$ value[3] (cm^{-1})
$p_\alpha{}^2$	2_{20}	F	7.56708175(35)	7.5652791(19)	7.5068034(55)
$(1/2)\ (1-\cos(3\alpha))$	2_{20}	V_3	407.59768(20)	407.91172(18)	407.58042(26)
$p_\alpha P_a$	2_{11}	ρ	0.328632673(20)	0.328300981(35)	0.322541154(65)
$P_a{}^2$	2_{02}	A_{RAM}	1.884881309(61)	1.88013742(13)	1.848976496(63)
$P_b{}^2$	2_{02}	B_{RAM}	0.348706489(16)	0.337726802(58)	0.348720666(61)
$P_c{}^2$	2_{02}	C_{RAM}	0.3031840478(44)	0.294817724(11)	0.302179145(18)
$\{P_a,P_b\}$	2_{02}	D_{ab}	−0.122669037(94)	−0.11817144(38)	−0.12175149(39)
$(1/2)\ (1-\cos(6\alpha))$	4_{40}	V_6	−11.63964(50)	-11.67172(20)	-11.71571(65)
$p_\alpha{}^4$	4_{40}	F_m	$-0.424416(38)\times10^{-3}$	$-0.427829(96)\times10^{-3}$	$-0.42834(12)\times10^{-3}$
$p_\alpha{}^3P_a$	4_{31}	ρ_m	$-0.832163(52)\times10^{-3}$	$-0.82821(11)\times10^{-3}$	$-0.81162(16)\times10^{-3}$
$P^2(1-\cos(3\alpha))$	4_{22}	V_{3J}	$0.5577894(41)\times10^{-3}$	$0.524776(16)\times10^{-3}$	$0.529795(22)\times10^{-3}$
$P_a{}^2(1-\cos(3\alpha))$	4_{22}	V_{3K}	$-0.19313906(98)\times10^{-1}$	$-0.1898291(17)\times10^{-1}$	$-0.1953217(29)\times10^{-1}$
$(P_b{}^2-P_c{}^2)(1-\cos(3\alpha))$	4_{22}	V_{3bc}	$0.2114597(52)\times10^{-3}$	$0.192215(19)\times10^{-3}$	$0.213208(15)\times10^{-3}$
$(1/2)\{P_a,P_b\}(1-\cos(3\alpha))$	4_{22}	V_{3ab}	$0.4235363(70)\times10^{-2}$	$0.405222(33)\times10^{-2}$	$0.443922(36)\times10^{-2}$
$p_\alpha{}^2P^2$	4_{22}	F_J	$-0.291704(53)\times10^{-5}$	$-0.26533(11)\times10^{-5}$	$-0.31536(19)\times10^{-5}$
$p_\alpha{}^2P_a{}^2$	4_{22}	F_K	$-0.982545(30)\times10^{-3}$	$-0.972792(46)\times10^{-3}$	$-0.944979(89)\times10^{-3}$
$p_\alpha{}^2(P_b{}^2-P_c{}^2)$	4_{22}	F_{bc}	$0.14720(12)\times10^{-5}$	$0.13745(31)\times10^{-5}$	$0.16632(37)\times10^{-5}$
$(1/2)\{P_a,P_c\}\sin(3\alpha)$	4_{22}	D_{3ac}	$-0.1405503(49)\times10^{-1}$	$-0.135881(17)\times10^{-1}$	$-0.142957(18)\times10^{-1}$
$(1/2)\{P_b,P_c\}\sin(3\alpha)$	4_{22}	D_{3bc}	$0.59173(13)\times10^{-3}$	$0.55489(43)\times10^{-3}$	$0.63859(48)\times10^{-3}$
$p_\alpha P_aP^2$	4_{13}	ρ_J	$0.958253(42)\times10^{-5}$	$0.91984(11)\times10^{-5}$	$0.91075(15)\times10^{-5}$
$p_\alpha P_a{}^3$	4_{13}	ρ_K	$-0.571407(12)\times10^{-3}$	$-0.564681(12)\times10^{-3}$	$-0.549548(31)\times10^{-3}$
$(1/2)\{P_a,(P_b{}^2-P_c{}^2)\}p_\alpha$	4_{13}	ρ_{bc}	$-0.5536(12)\times10^{-6}$	$-0.5763(36)\times10^{-6}$	$-0.2887(35)\times10^{-6}$
$-P^4$	4_{04}	Δ_J	$0.3244101(54)\times10^{-6}$	$0.306742(20)\times10^{-6}$	$0.325255(24)\times10^{-6}$
$-P^2P_a{}^2$	4_{04}	Δ_{JK}	$-0.581770(50)\times10^{-5}$	$-0.556079(86)\times10^{-5}$	$-0.571647(79)\times10^{-5}$
$-P_a{}^4$	4_{04}	Δ_K	$0.1308173(26)\times10^{-3}$	$0.1292582(29)\times10^{-3}$	$0.1263888(56)\times10^{-3}$
$-2P^2(P_b{}^2-P_c{}^2)$	4_{04}	δ_J	$0.778472(23)\times10^{-7}$	$0.709225(70)\times10^{-7}$	$0.786517(69)\times10^{-7}$
$-\{P_a{}^2,(P_b{}^2-P_c{}^2)\}$	4_{04}	δ_K	$0.94268\ (17)\times10^{-6}$	$0.105094(90)\times10^{-5}$	$0.10255(12)\times10^{-5}$
$\{P_a,P_b\}P^2$	4_{04}	D_{abJ}	$0.867443(32)\times10^{-6}$	$0.81273(20)\times10^{-6}$	$0.85179(14)\times10^{-6}$
$\{P_a{}^3,P_b\}$	4_{04}	D_{abK}	$0.30498(25)\times10^{-5}$	$0.29239(46)\times10^{-5}$	$0.27116(33)\times10^{-5}$
$(1/2)\ (1-\cos(9\alpha))$	6_{60}	V_9	−0.20318(11)	−0.14153(11)	−0.2413(14)
$p_\alpha{}^6$	6_{60}	F_{mm}	$-0.5066(16)\times10^{-6}$	$-0.8986(20)\times10^{-6}$	$-0.7480(55)\times10^{-6}$
$p_\alpha{}^5P_a$	6_{51}	ρ_{mm}	$-0.7147(34)\times10^{-6}$	$-0.14955(33)\times10^{-5}$	$-0.1138(11)\times10^{-5}$
$P^2(1-\cos(6\alpha))$	6_{42}	V_{6J}	$0.557997(73)\times10^{-4}$	$0.54132(35)\times10^{-4}$	$0.58065(59)\times10^{-4}$
$P_a{}^2(1-\cos(6\alpha))$	6_{42}	V_{6K}	$-0.37191(19)\times10^{-3}$	$-0.37805(54)\times10^{-3}$	$-0.33899(20)\times10^{-3}$
$(1/2)\{P_a,P_b\}(1-\cos(6\alpha))$	6_{42}	V_{6ab}	$-0.13638(10)\times10^{-3}$	$-0.12574(40)\times10^{-3}$	$-0.12853(37)\times10^{-3}$
$(P_b{}^2-P_c{}^2)(1-\cos(6\alpha))$	6_{42}	V_{6bc}	–	$0.1222(48)\times10^{-5}$	$-0.829(29)\times10^{-6}$
$p_\alpha{}^4P^2$	6_{42}	F_{mJ}	$-0.1259(18)\times10^{-9}$	–	$-0.4837(88)\times10^{-8}$
$p_\alpha{}^4P_a{}^2$	6_{42}	F_{mK}	$-0.1712(36)\times10^{-6}$	$-0.8131(17)\times10^{-6}$	$-0.5599(92)\times10^{-6}$
$p_\alpha{}^4(P_b{}^2-P_c{}^2)$	6_{42}	F_{mbc}	$0.1197(22)\times10^{-8}$	–	–
$(1/2)\{P_b,P_c\}\sin(6\alpha)$	6_{42}	D_{6bc}	$-0.72949(57)\times10^{-4}$	$-0.6730(24)\times10^{-4}$	$-0.7137(16)\times10^{-4}$
$(1/2)\{P_a,P_c\}\sin(6\alpha)$	6_{42}	D_{6ac}	$0.46097(67)\times10^{-3}$	$0.4258(12)\times10^{-3}$	$0.5301(10)\times10^{-3}$
$(1/2)\{P_a,P_c,p_\alpha{}^2,\sin(3\alpha)\}$	6_{42}	D_{3acm}	$-0.3178(66)\times10^{-5}$	–	–
$p_\alpha{}^3P_a{}^3$	6_{33}	ρ_{mK}	$0.2946(23)\times10^{-6}$	–	$0.754(45)\times10^{-7}$
$p_\alpha{}^3P_aP^2$	6_{33}	ρ_{mJ}	$-0.5306(26)\times10^{-8}$	$-0.3235(44)\times10^{-8}$	$-0.968(12)\times10^{-8}$
$(1/2)\{P_a,P_b,P_c,p_\alpha,\sin(3\alpha)\}$	6_{33}	ρ_{3bc}	$0.47689(54)\times10^{-5}$	–	–
$(1/2)\{P_a,(P_b{}^2-P_c{}^2)\}p_\alpha{}^3$	6_{33}	ρ_{mbc}	$0.4347(38)\times10^{-8}$	$-0.995(35)\times10^{-9}$	–
$P^4(1-\cos(3\alpha))$	6_{24}	V_{3JJ}	$-0.77602(42)\times10^{-8}$	$-0.4499(21)\times10^{-8}$	$-0.5065(25)\times10^{-8}$
$P^2P_a{}^2(1-\cos(3\alpha))$	6_{24}	V_{3JK}	–	$-0.23620(40)\times10^{-6}$	–
$P_a{}^4(1-\cos(3\alpha))$	6_{24}	V_{3KK}	$0.115646(94)\times10^{-5}$	$0.11145(17)\times10^{-5}$	$0.12880(30)\times10^{-5}$
$p_\alpha{}^2P^4$	6_{24}	F_{JJ}	–	$0.2343(39)\times10^{-10}$	$0.1768(58)\times10^{-10}$
$p_\alpha{}^2P^2P_a{}^2$	6_{24}	F_{JK}	$-0.6904(18)\times10^{-8}$	$-0.5620(48)\times10^{-8}$	$-0.9637(65)\times10^{-8}$
$p_\alpha{}^2P_a{}^4$	6_{24}	F_{KK}	$0.30324(86)\times10^{-6}$	$0.22248(28)\times10^{-6}$	$0.2220(15)\times10^{-6}$
$P^2(P_b{}^2-P_c{}^2)(1-\cos(3\alpha))$	6_{24}	V_{3bcJ}	$-0.17920(30)\times10^{-8}$	–	$-0.2040(11)\times10^{-8}$
$(1/2)\{P_a{}^3,P_c\}\sin(3\alpha)$	6_{24}	D_{3acK}	$0.1246(10)\times10^{-5}$	$0.1141(18)\times10^{-5}$	$0.171(10)\times10^{-6}$
$(1/2)\{P_a,P_c\}P^2\sin(3\alpha)$	6_{24}	D_{3acJ}	$0.10821(34)\times10^{-7}$	$0.7636(98)\times10^{-7}$	$0.372(14)\times10^{-7}$
$(1/2)\{P_b,P_c\}P^2\sin(3\alpha)$	6_{24}	D_{3bcJ}	$-0.7436(17)\times10^{-8}$	$-0.6126(43)\times10^{-8}$	$-0.5837(99)\times10^{-8}$

Notes. [1] $\{A,B\}=AB+BA$; $\{A,B,C\}=ABC+CBA$; $\{A,B,C,D\}=ABCD+DCBA$. The product of the operator in the first column of a given row and the parameter in the third column of that row gives the term actually used in the torsion-rotation Hamiltonian of the program, except for F, ρ, and A_{RAM}, which occur in the Hamiltonian in the form $F(P_\alpha+\rho P_a)^2+A_{RAM}P_a^2$. [2] $n=t+r$, where n is the total order of the operator, t is the order of the torsional part, and r is the order of the rotational part, respectively. [3] All values are in cm^{-1}, except ρ which is unitless. Statistical uncertainties are shown as one standard uncertainty in the units of the last two digits.

Table 7. continued.

Operator[1]	n_{tr}[2]	Parameter	$^{12}CH_3{}^{12}CHO$ value[3] (cm^{-1})	$^{13}CH_3{}^{12}CHO$ value[3] (cm^{-1})	$^{12}CH_3{}^{13}CHO$ value[3] (cm^{-1})
$(1/2)\{P_a{}^2,P_b,P_c\}\sin(3\alpha)$	6_{24}	D_{3bcK}	$0.14846(12)\times10^{-5}$	$-0.2309(55)\times10^{-6}$	$-0.713(55)\times10^{-7}$
$(1/2)(\{P_a,P_b{}^3\}-\{P_a,P_b,P_c{}^2\})\cos(3\alpha)$	6_{24}	V_{3ab3}	$0.38167(73)\times10^{-7}$	$0.5101(22)\times10^{-7}$	$0.5078(27)\times10^{-7}$
$P^2P_a{}^2(1-\cos(3\alpha))$	6_{24}	V_{3JK}	$-0.23880(36)\times10^{-6}$	–	$-0.28455(63)\times10^{-6}$
$(1/2)\{P_a,P_b\}P^2(1-\cos(3\alpha))$	6_{24}	V_{3abJ}	–	$-0.566(26)\times10^{-8}$	–
$(1/2)\{P_a{}^3,P_b\}(1-\cos(3\alpha))$	6_{24}	V_{3abK}	$0.1562(36)\times10^{-6}$	$0.2057(47)\times10^{-6}$	$0.4345(43)\times10^{-6}$
$P^2(P_b{}^2-P_c{}^2)(1-\cos(3\alpha))$	6_{24}	V_{3bcJ}	–	$-0.1586(11)\times10^{-8}$	–
$(1/2)\{P_a{}^2,(P_b{}^2-P_c{}^2)\}(1-\cos(3\alpha))$	6_{24}	V_{3bcK}	–	$0.28389(89)\times10^{-6}$	$0.2838(15)\times10^{-6}$
$(1/2)\{P_a,P_c{}^3\}\sin(3\alpha)$	6_{24}	D_{3ac3}	$-0.3543(24)\times10^{-7}$	$-0.3397(69)\times10^{-7}$	–
$(1/2)(\{P_b{}^3,P_c\}-\{P_b,P_c{}^3\})\sin(3\alpha)$	6_{24}	D_{3bc3}	–	$-0.2447(29)\times10^{-8}$	$-0.2554(33)\times10^{-8}$
$p_\alpha{}^2(P_b{}^2-P_c{}^2)P^2$	6_{24}	F_{bcJ}	–	–	$0.1505(72)\times10^{-10}$
$(1/2)\{P_a{}^2,(P_b{}^2-P_c{}^2)\}p_\alpha{}^2$	6_{24}	F_{bcK}	$0.7853(30)\times10^{-8}$	–	–
$p_\alpha{}^2(P_c{}^4+P_b{}^4)$	6_{24}	F_{b2c2}	$0.49528(94)\times10^{-10}$	–	–
$(P_b{}^4+P_c{}^4)\cos3a$	6_{24}	V_{3b2c2}	$-0.32294(69)\times10^{-8}$	$0.770(22)\times10^{-9}$	$0.684(31)\times10^{-9}$
$p_\alpha P_a P^4$	6_{15}	ρ_{JJ}	–	–	$-0.2008(54)\times10^{-10}$
$p_\alpha P_a{}^3P^2$	6_{15}	ρ_{JK}	$-0.40507(54)\times10^{-8}$	$-0.3627(21)\times10^{-8}$	$-0.4479(25)\times10^{-8}$
$p_\alpha P_a{}^5$	6_{15}	ρ_{KK}	$0.12126(20)\times10^{-6}$	$0.10832(11)\times10^{-6}$	$0.10436(34)\times10^{-6}$
$(1/2)\{P_a,(P_b{}^2-P_c{}^2)\}P^2p_\alpha$	6_{15}	ρ_{bcJ}	$-0.15285(93)\times10^{-10}$	–	–
$(1/2)\{P_a{}^3,(P_b{}^2-P_c{}^2)\}p_\alpha$	6_{15}	ρ_{bcK}	$0.6381(14)\times10^{-8}$	$0.1989(33)\times10^{-8}$	$0.1085(16)\times10^{-8}$
$\{P_a,P_b\}P^4$	6_{06}	D_{abJJ}	$-0.16905(91)\times10^{-11}$	$-0.1419(35)\times10^{-11}$	–
$\{P_a{}^3,P_b\}P^2$	6_{06}	D_{abJK}	$0.8607(65)\times10^{-10}$	$0.478(19)\times10^{-10}$	$0.3802(27)\times10^{-9}$
$\{P_a{}^5,P_b\}$	6_{06}	D_{abKK}	$0.11154(82)\times10^{-8}$	$0.888(24)\times10^{-9}$	$0.4607(23)\times10^{-8}$
P^6	6_{06}	Φ_J	$0.80483(59)\times10^{-12}$	$0.6874(26)\times10^{-12}$	$0.7043(10)\times10^{-12}$
$P^4P_a{}^2$	6_{06}	Φ_{JK}	$-0.2732(10)\times10^{-10}$	$-0.1630(29)\times10^{-10}$	$-0.4677(31)\times10^{-10}$
$P^2P_a{}^4$	6_{06}	Φ_{KJ}	$-0.14266(25)\times10^{-8}$	$-0.12937(55)\times10^{-8}$	$-0.17957(56)\times10^{-8}$
$P_a{}^6$	6_{06}	Φ_K	$0.19759(23)\times10^{-7}$	$0.18596(18)\times10^{-7}$	$0.18908(47)\times10^{-7}$
$2P^4(P_b{}^2-P_c{}^2)$	6_{06}	ϕ_J	$0.38476(25)\times10^{-12}$	$0.3246(12)\times10^{-12}$	$0.34399(69)\times10^{-12}$
$P^2\{P_a{}^2,(P_b{}^2-P_c{}^2)\}$	6_{06}	ϕ_{JK}	$-0.9470(55)\times10^{-11}$	$-0.653(13)\times10^{-11}$	$-0.1633(14)\times10^{-10}$
$\{P_a{}^4,(P_b{}^2-P_c{}^2)\}$	6_{06}	ϕ_K	$0.54529(21)\times10^{-9}$	$0.3514(59)\times10^{-9}$	–
$(1/2)\ (1-\cos(12\alpha))$	8_{80}	V_{12}	0.10123(15)	–	0.1718(18)
$p_\alpha{}^8$	8_{80}	F_{mmm}	$-0.8628(32)\times10^{-8}$	–	–
$p_\alpha{}^7P_a$	8_{71}	ρ_{mmm}	$-0.20698(86)\times10^{-7}$	–	–
$P^2(1-\cos(9\alpha))$	8_{62}	V_{9J}	$-0.15703(56)\times10^{-5}$	$-0.1211(24)\times10^{-5}$	$-0.3590(49)\times10^{-5}$
$P_a{}^2(1-\cos(9\alpha))$	8_{62}	V_{9K}	$0.3044(14)\times10^{-4}$	$0.4013(45)\times10^{-4}$	–
$(P_b{}^2-P_c{}^2)(1-\cos(9\alpha))$	8_{62}	V_{9bc}	$-0.11444(53)\times10^{-5}$	$-0.1967(52)\times10^{-5}$	–
$(1/2)\{P_a,P_b\}(1-\cos(9\alpha))$	8_{62}	V_{9ab}	–	$-0.608(35)\times10^{-5}$	$-0.599(34)\times10^{-5}$
$(1/2)\{P_a,P_c\}\sin(9\alpha)$	8_{62}	D_{9ac}	–	$0.1409(39)\times10^{-4}$	–
$(1/2)\{P_b,P_c\}\sin(9\alpha)$	8_{62}	D_{9bc}	$0.884(13)\times10^{-6}$	–	$-0.343(10)\times10^{-5}$
$P_a{}^2p_\alpha{}^6$	8_{62}	F_{mmK}	$-0.2202(11)\times10^{-7}$	$-0.1406(33)\times10^{-9}$	–
$(1/2)\{P_a,P_b\}p_\alpha{}^6$	8_{62}	F_{mmab}	$0.2906(29)\times10^{-10}$	–	–
$P_a{}^3p_\alpha{}^5$	8_{53}	ρ_{mmK}	$-0.13762(98)\times10^{-7}$	–	–
$p_\alpha{}^4P_a{}^4$	8_{44}	F_{mKK}	$-0.5734(57)\times10^{-8}$	–	–
$(1/2)P^2\{P_a,P_c\}\sin(6\alpha)$	8_{44}	D_{6acJ}	$-0.6552(93)\times10^{-8}$	–	–
$(1/2)\{P_a{}^3,P_c\}\sin(6\alpha)$	8_{44}	D_{6acK}	–	–	$0.425(37)\times10^{-7}$
$(1/2)\{P_b,P_c\}P^2\sin(6\alpha)$	8_{44}	D_{6bcJ}	$0.6210(71)\times10^{-9}$	$0.748(21)\times10^{-9}$	–
$(1/2)(\{P_b{}^3,P_c\}-\{P_b,P_c{}^3\})\sin(6\alpha)$	8_{44}	D_{6bc3}	–	$0.5148(97)\times10^{-9}$	$0.996(12)\times10^{-9}$
$P^4(1-\cos(6\alpha))$	8_{44}	V_{6JJ}	$-0.799(16)\times10^{-10}$	–	–
$P_a{}^4(1-\cos(6\alpha))$	8_{44}	V_{6KK}	$0.15152(47)\times10^{-6}$	$0.1380(11)\times10^{-6}$	$0.1679(26)\times10^{-6}$
$(1/2)\{P_a,P_b\}P^2(1-\cos(6\alpha))$	8_{44}	V_{6abJ}	–	$-0.554(14)\times10^{-8}$	–
$(1/2)\{P_a{}^3,P_b\}(1-\cos(6\alpha))$	8_{44}	V_{6abK}	$-0.6966(58)\times10^{-7}$	$-0.542(21)\times10^{-7}$	–
$P^2(P_b{}^2-P_c{}^2)(1-\cos(6\alpha))$	8_{44}	V_{6bcJ}	–	–	$-0.2303(65)\times10^{-9}$
$(1/2)(\{P_a,P_b{}^3\}-\{P_a,P_b,P_c{}^2\})\cos(6\alpha)$	8_{44}	V_{6ab3}	–	$-0.430(16)\times10^{-8}$	–
$p_\alpha{}^3P_aP^4$	8_{35}	ρ_{mJJ}	–	$-0.873(21)\times10^{-13}$	–
$p_\alpha{}^3P_a{}^5$	8_{35}	ρ_{mKK}	$-0.1656(23)\times10^{-8}$	–	–
$(1/2)\{P_a,P_b{}^3,P_c,p_\alpha,\sin(3\alpha)\}-(1/2)\{P_a,P_b,P_c{}^3,p_\alpha,\sin(3\alpha)\}$	8_{35}	ρ_{3bc3}	$-0.2511(23)\times10^{-10}$	–	–
$P^6(1-\cos(3\alpha))$	8_{26}	V_{3JJJ}	$0.1344(25)\times10^{-13}$	–	–
$P^4P_a{}^2(1-\cos(3\alpha))$	8_{26}	V_{3JJK}	$0.3715(39)\times10^{-11}$	–	–
$P^2P_a{}^4(1-\cos(3\alpha))$	8_{26}	V_{3JKK}	$0.472(13)\times10^{-10}$	$0.303(11)\times10^{-10}$	–
$(1/2)P^2\{P_a{}^3,P_b\}(1-\cos(3\alpha))$	8_{26}	V_{3abJK}	–	$0.3426(55)\times10^{-10}$	–
$(1/2)\{P_a{}^5,P_b\}(1-\cos(3\alpha))$	8_{26}	V_{3abKK}	$-0.2031(61)\times10^{-9}$	–	–
$(1/2)P^2\{P_a{}^3,P_c\}\sin(3\alpha)$	8_{26}	D_{3acJK}	$-0.5470(82)\times10^{-10}$	–	–
$(1/2)\{P_a{}^5,P_c\}\sin(3\alpha)$	8_{26}	D_{3acKK}	–	$0.450(27)\times10^{-10}$	–

Table 7. continued.

Operator[1]	n_{tr}[2]	Parameter	$^{12}CH_3{}^{12}CHO$ value[3] (cm^{-1})	$^{13}CH_3{}^{12}CHO$ value[3] (cm^{-1})	$^{12}CH_3{}^{13}CHO$ value[3] (cm^{-1})
$(1/2)P^2\{P_a{}^2,P_b,P_c\}\sin(3\alpha)$	8_{26}	D_{3bcJK}	$0.854(18)\times10^{-11}$	–	–
$(1/2)\{P_a{}^4,P_b,P_c\}\sin(3\alpha)$	8_{26}	D_{3bcKK}	–	–	$-0.1697(63)\times10^{-9}$
$(1/2)\{P_a{}^3,P_c{}^3\}\sin(3\alpha)$	8_{26}	D_{3ac3K}	$0.6486(74)\times10^{-10}$	–	–
$p_\alpha{}^2P_a{}^6$	8_{26}	F_{KKK}	$-0.3325(57)\times10^{-9}$	–	–
$p_\alpha P_a{}^3P^4$	8_{17}	ρ_{JJK}	–	–	$0.842(43)\times10^{-13}$
$p_\alpha P_a{}^7$	8_{17}	ρ_{KKK}	$-0.4300(86)\times10^{-10}$	–	$-0.353(15)\times10^{-11}$
P^8	8_{08}	L_J	$-0.3808(46)\times10^{-17}$	$-0.358(24)\times10^{-17}$	–
$P^4P_a{}^4$	8_{08}	L_{JK}	$0.5000(60)\times10^{-14}$	–	$0.372(14)\times10^{-13}$
$P_a{}^8$	8_{08}	L_K	$-0.2743(71)\times10^{-11}$	–	$-0.1256(48)\times10^{-11}$
$2P^6(P_b{}^2-P_c{}^2)$	8_{08}	l_J	$-0.1626(22)\times10^{-17}$	$-0.1332(63)\times10^{-17}$	$-0.1426(83)\times10^{-17}$
$p_\alpha{}^8P_a{}^2$	10_{82}	F_{mmmK}	–	$0.281(16)\times10^{-12}$	–
$(1/2)P^2\{P_a,P_b\}(1-\cos(9\alpha))$	10_{64}	V_{9abJ}	$-0.1960(28)\times10^{-8}$	–	–
$P^4P_a{}^2(1-\cos(6\alpha))$	10_{46}	V_{6JJK}	–	–	$0.3164(60)\times10^{-11}$
$P^2P_a{}^4(1-\cos(6\alpha))$	10_{46}	V_{6JKK}	–	–	$-0.222(11)\times10^{-10}$
$(1/2)\{P_a{}^5,P_b\}(1-\cos(6\alpha))$	10_{46}	V_{6abKK}	$-0.585(13)\times10^{-10}$	–	–
$p_\alpha{}^2P_a{}^8$	10_{28}	F_{KKKK}	$0.1427(47)\times10^{-14}$	–	–

Table 8. Torsion-rotation part $Qrt(T)$ of the total internal partition function $Q(T) = Qv(T) * Qrt(T)$, calculated from first principles using the parameter set of Table 7.

	$^{13}CH_3CHO$			$CH_3{}^{13}CHO$		
T(K)	Qrt (A+E)	Qrt (A)	Qrt (E)	Qrt (A+E)	Qrt (A)	Qrt (E)
10	153.249	76.8662	77.1410	150.384	75.4230	75.6797
20	431.553	215.993	216.626	423.373	211.895	212.489
30	792.543	396.437	397.413	777.474	388.897	389.814
40	1225.44	612.827	614.125	1202.20	601.205	602.429
50	1730.87	865.497	867.088	1698.28	849.196	850.700
60	2314.40	1157.23	1159.08	2271.23	1135.64	1137.39
70	2983.09	1491.56	1493.64	2928.03	1464.02	1466.00
80	3744.16	1872.08	1874.39	3675.80	1837.90	1840.09
90	4604.57	2302.29	2304.81	4521.40	2260.70	2263.10
100	5570.85	2785.43	2788.18	5471.25	2735.63	2738.24
110	6649.03			6531.29		
120	7844.64			7706.97		
130	9162.72			9003.25		
140	10 607.9			10 424.6		
150	12 184.2			11 975.2		
160	13 895.5			13 658.7		
170	15 745.0			15 478.4		
180	17 736.0			17 437.3		
190	19 871.0			19 538.1		
200	22 152.6			21 783.2		
210	24 583.1			24 174.9		
220	27 164.3			26 715.1		
230	29 898.2			29 405.7		
240	32 786.3			32 248.1		
250	35 830.2			35 243.9		
260	39 031.0			38 394.3		
270	42 390.1			41 700.5		
280	45 908.4			45 163.4		
290	49 586.8			48 784.1		
300	53 426.1			52 563.2		

Notes. For the temperatures below 100 K, the separate A and E parts of the torsion-rotation part of partition function are given, where the A and E type levels are treated as the independent subsets of energy levels. The vibrational part $Qv(T)$ (omitting the torsional vibration since it is taken into account in Qrt) may be estimated in the harmonic approximation using the vibrational frequencies reported for the parent species of acetaldehyde by Schimanouchi, Tables of Molecular Vibrational Frequencies, Vol. I: consolidated (National Bureau of Standards, Washington, DC, 1972), pp. 1160. In the calculation the states up to $J = 100$ and $vt = 8$ were included.

acetaldehydes. Using the RAM Hamiltonian models, we were able to fit the available data within experimental accuracy. The results of the present study allowed us to produce reliable predictions of rotational spectra in the ground and first excited torsional states of $^{13}CH_3CHO$ and $CH_3{}^{13}CHO$ isotopologs for astrophysical purposes in the frequency range up to 1 THz for $0 < J < 65$ and $0 < K_a < 20$.

Acknowledgements. This work was done with the support of the Ukrainian-French CNRS-PICS 6051 project. The Centre National d'Etudes Spatiales (CNES) and the Action sur Projets de l'INSU, "Physique et Chimie du Milieu Interstellaire" are acknowledged for financial support. This work was also done under the ANR-08-BLAN-0054.

References

Alekseev, E. A., Motiyenko, R. A., & Margulès, L. 2012, Radio Physics Radio Astronomy, 3, 75
Barbry, D., & Couturier, D. J. 1987, Labelled Comp. Radiopharm., XXIV, 603
Bouchez, A., Margulès, L., Motiyenko, R. A., et al. 2012, A&A, 540, A51
Carvajal, M., Margulès, L., Tercero, B., et al. 2009, A&A, 500, 1109
Charnley, S. B. 2004, Adv. Space Res., 33, 23
Coudert, L. H., Margulès, L., Huet, T. R., et al. 2012, A&A, 543, A46
Coudert, L. H., Drouin, B. J., Tercero, B., et al. 2013, ApJ, 779, 119
Demyk, K., Mäder, H., Tercero, B., et al. 2007, A&A, 466, 255
Elkeurti, M., Coudert, L. H., Medvedev, I. R., et al. 2010, J. Mol. Spectr., 263, 145
Gordy, W., & Cook, R. L. 1984, Microwave Molecular Spectra, Techniques of Chemistry, Vol. XVIII (New York: Wiley)
Haykal, I., Motiyenko, R. A., Margulès, L., & Huet, T. R. 2013, A&A, 549, A96
Herbst, E., Messer, J. K., De Lucia, F. C., & Helminger, P. 1984, J. Mol. Spectr., 108, 42
Hougen, J. T., Kleiner, I., & Godefroid, M. 1994, J. Mol. Spectr., 163, 559
Ilyushin, V. V., Kisiel, Z., Pszczólkowski, L., Mäder, H., & Hougen, J. T. 2010, J. Mol. Spectr., 259, 26
Ilyushin, V. V., Endres, C. P., Lewen, F., Schlemmer, S., & Drouin, B. J. 2013, J. Mol. Spectr., 290, 31
Kilb, R. W., Lin, C. C., & Wilson, E. B. 1957 J. Chem. Phys., 26, 1695
Kirtman, B. 1962, J. Chem. Phys., 37, 2516
Kleiner, I. 2010, J. Mol. Spectr., 260, 1
Kutsenko, A. S., Motiyenko, R. A., Margulès, L., & Guillemin, J.-C. 2013, A&A, 549, A128
Lees, R. M., & Baker, J. G. 1968, J. Chem. Phys., 48, 5299
Margulès, L., Motiyenko, R. A., Demyk, K., et al. 2009a, A&A, 493, 565
Margulès, L., Coudert, L. H., Møllendal, H., et al. 2009b, J. Mol. Spectr., 254, 55
Margulès, L., Huet, T. R., Demaison, J., et al. 2010, ApJ, 714, 1120
Martinache, L., & Bauder, A. 1989, Chem. Phys. Lett., 164, 657
Matthews, H. E., Friberg, P., & Irvine, W. M. 1985, ApJ, 290, 609
Muller, S., Beelen, A., Guelin, M., et al. 2011, A&A, 535, A103
Nguyen, L., Walters, A., Margulès, L., et al. 2013, A&A, 553, A84
Nummelin, A., Dickens, J. E., Bergman, P., et al. 1998, A&A, 337, 275
Richard, C., Margulès, L., Motiyenko, R. A., & Guillemin, J.-C. 2012, A&A, 543, A135
Richard, C., Margulès, L., Caux, E., et al. 2013, A&A, 552, A117
Schimanouchi, T. 1972, in Tables of Molecular Vibrational Frequencies, Vol. I: consolidated (Washington, DC: National Bureau of Standards), 89
Smirnov, I. A., Alekseev, E. A., Ilyushin, V. V., et al. 2014, J. Mol. Spectr., 295, 44
Tercero, B., Margulès, L., Carvajal, M., et al. 2012, A&A, 538, A119
Turner, P. M., & Cox, A. P. 1976, Chem. Phys. Lett., 42, 84
Turner, P. M., Cox, A. P., & Hardy, J. A. 1981, J. Chem. Soc. Faraday Trans. 2, 77, 1217
Turner, B. E., Terzieva, R., & Herbst, E. 1999, ApJ, 518, 699
Zaleski, D. P., Neill, J. L., Muckle, M. T., et al. 2012, J. Mol. Spectr., 280, 68